Macromolecules
ARTICLE

Macromolecules **2010**, *43*, 1907–1914 **1907**
DOI: 10.1021/ma9026383

A Dielectric Study of Oligo- and Poly(propylene glycol)

Catalin Gainaru,*,† Wolf Hiller,‡ and Roland Böhmer†

†*Fakultät für Physik, Technische Universität Dortmund, 44221 Dortmund, Germany, and*
‡*Fakultät für Chemie, Technische Universität Dortmund, 44221 Dortmund, Germany*

Received December 2, 2009; Revised Manuscript Received January 15, 2010

ABSTRACT: The segmental and normal mode dynamics of poly(propylene glycol) (PPG) were studied using dielectric spectroscopy for a wide range of molecular weights. For intermediate chain lengths the normal mode spectra, unmasked by electrical purging procedures, were described quantitatively using the Rouse model. Based on the ratio of the dispersion strengths of the normal and of the segmental mode, the characteristic ratio C_∞ was determined. The spectral width of the segmental mode evolves smoothly with the number of repeat units N and, except for dipropylene glycol, so does the mean time scale. The exceptional behavior was confirmed by ^{13}C NMR relaxation experiments. For small N the segmental and the normal modes tend to merge near the glass transformation range. Exploiting the polymer chains as "molecular rulers", the growth of the characteristic length scale associated with the vitrification process is estimated for PPG. In the glassy state two dipolarly active relaxation processes were resolved. The slower one is characterized by an activation energy typical for hydrated systems, and its dispersion strength can be modified by appropriate heat treatment.

I. Introduction

Without changing the chemical constitution, oligomeric and polymeric melts allow one to study variations of structural and dynamical processes which span wide ranges of length scales. When increasing the chain length, starting from just a few repeat units, it is an important question at which molecular weight M_w the (macro)molecule develops the typical characteristics of a polymer.[1−7] When the chains become longer, they reveal scaling properties which can be described by the Rouse model and its refinements until eventually the chains tend to entangle and find themselves confined and reptating in transient tubes.[8,9] Apart from the segmental dynamics, one is often interested in studying motional processes on the scale of the polymer's end-to-end distance. This global scale can be accessed most easily via the normal mode in dielectric spectroscopy[10,11] *if* the segments of the polymer under consideration exhibit an electrical dipole moment along the chain contour. Representatives of this class of so-called type A polymers are poly(isoprene) (PI),[12] poly(oxyethylene),[13] poly(oxybutylene),[14] and poly(lactide)[15] to name a few.[16] Because of the simultaneous presence of C and O atoms in the polymer backbone, also poly(propylene glycol) (PPG), which is in the focus of the current work, features a molecular weight dependent end-to-end dipole moment arising from the vector summation of these longitudinal segmental dipole moments.[1]

PPG molecules with different degrees of polymerization N were studied by a number of techniques including dielectric spectroscopy,[2,17−22,28] calorimetry,[22] field gradient diffusometry,[24,25] the Kerr effect,[2] various light scattering methods,[18,24,26−29] mechanical and ultrasonic experiments,[30,31] neutron scattering,[32] and NMR.[33] Furthermore, studies were conducted with PPG exposed to high pressures[34] or to spatial confinement.[23,35,36] In the bulk the entanglement molecular weight of PPG is about $M_e \approx$ 5300 g/mol,[37] corresponding to $N_e = 90$ repeat units, although somewhat different estimates were also given.[25,38] The OH groups in PPG can mediate hydrogen bonding which leads to transient entanglements.[25,39,40] Furthermore, the PPG system exhibits a relatively weak dependence of T_g on the number of monomer units.[18,22] That this peculiar behavior is due to H-bonding was convincingly demonstrated in studies in which the terminal groups of the PPG chains were chemically altered: For those "end-capped" macromolecules[18,20] the glass transition temperatures saturated much more slowly with increasing chain length.

In this article we are not primarily concerned with the change of properties when going from the Rouse regime to the domain governed by entanglements. Merely, we address the question what happens when entering the polymeric state by systematically increasing the chain length starting from the low-molecular-weight, even single monomer unit. Monomeric propylene glycol (PG) as well as dipropylene glycol (2PG) and tripropylene glycol (3PG) were studied using dielectric measurements.[41−44] Here we examine the samples with $N = 1$, 2, and 3 also using ^{13}C NMR spin−lattice relaxation experiments. Clearly, 3PG is too short to be considered a polymer but beyond which molecular weight is a polymer a polymer? It is customary to define the onset of polymeric behavior by the establishment of random walk statistics for the chain conformations. For PPG we demonstrated recently that this is the case for N of about 30.[37] The Gaussian regime was recognized by the fact that here the ratio of the dispersion strengths of the normal mode to that of the segmental mode (α-process) is expected to be independent of N.

This paper extends our previous investigations[37] of PPG, and it is organized as follows: After giving some experimental details, in section III.A we focus attention on the dielectric normal mode, i.e., on relaxation processes slower than the segmental motion. Then, in section III.B we deal with this motion itself mostly focusing on the low-M_w regime in which polymer behavior sets in. Section III.C is devoted to a discussion of relaxations faster than the segmental motion. Finally, in section III.D we demonstrate how the end-to-end distance can be used as a molecular ruler to estimate the cooperativity length scale at the glass transition of PPG. A discussion of various aspects (section IV) and a summary (section V) conclude this article.

*To whom correspondence should be addressed.

Published on Web 02/01/2010

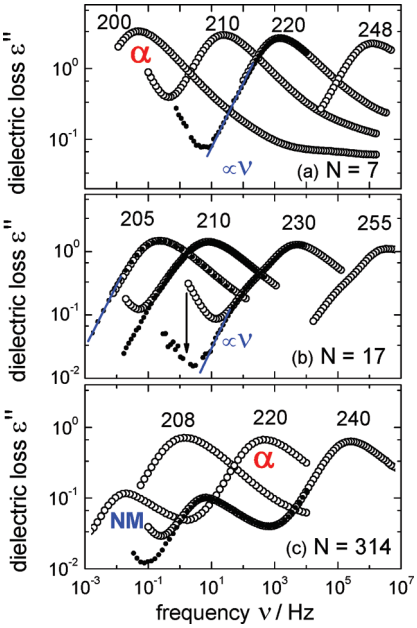

Figure 1. Dielectric loss spectra for PPG with $N = 7$, 17, and 314 repeat units measured at the temperatures given in kelvin. The straight lines mark the slope $\varepsilon'' \propto \nu^1$. For the heptamer the loss is typical for that of a low-molecular-weight glass former. The low-frequency flank of ε'' for the $N = 17$ sample reveals a linear increase only after applying electrical purging (filled symbols). The change of positive slope of the low-frequency flank is indicative for polymeric behavior. The macromolecular sample ($N = 314$) exhibits a fully developed normal mode peak.

II. Experimental Details

PG and 2PG were purchased from Fluka and 3PG from Aldrich. PPG samples with $N = 7$, 13, 17, 35, 52, and 93 were received from PSS Mainz, and polymers with high molecular weights ($N = 214$ and 314) were kindly provided by Bayer Co. Thus, overall the range 76 g/mol $\leq M_w \leq$ 18 200 g/mol was covered. Information regarding the polydispersity of the samples was given previously.[37] All samples were stored under dry, dark, and cold conditions and used without further chemical treatment.

Measurements of the complex dielectric constant $\varepsilon^* = \varepsilon' - i\varepsilon''$ were conducted using an α-analyzer from Novocontrol in the frequency range 10^{-3} Hz $\leq \nu \leq 10^7$ Hz. The parallel-plate dielectric cell, made of sapphire and invar steel,[45] had a geometrical capacitance of 20 pF and an electrode separation of 100 μm. Variable temperature measurements of ^{13}C spin−lattice relaxation times were carried at a Larmor frequency of $\omega_C = 2\pi \times$ 75 MHz using a Bruker DXP spectrometer. For all measurements the temperature was stabilized within ±0.2 K.

III. Results

A. Relaxation Slower Than the Segmental Dynamics: Dielectric Normal Modes. To gain an overview on the dynamical behavior of oligomeric and polymeric propylene glycol, in Figure 1 we present dielectric loss spectra for the species with $N = 7$, 17, and 314. For the heptamer typical features of a supercooled liquid are recognized. The main peak, corresponding to the structural process, also called α-relaxation, is slightly asymmetrically broadened on the logarithmic frequency axis. The low-ν side of the loss peak can be described by a power law $\varepsilon'' \propto \nu^\alpha$ with $\alpha = 1$. For $N = 17$ the segmental relaxation peaks are somewhat broader, and at a given temperature, they are shifted to higher frequencies. As a signature of the polymer dynamics, emerging as a consequence of the slightly increased chain length, the power law exponent characterizing the low-frequency side in the immediate vicinity of the loss peak becomes smaller, $\alpha < 1$. At still lower frequencies a power law regime $\varepsilon'' \propto \nu^1$ exists which stems from chain modes, as will be discussed below. Finally, for much longer chains the dielectric normal mode shows up as a fully developed low-frequency peak.

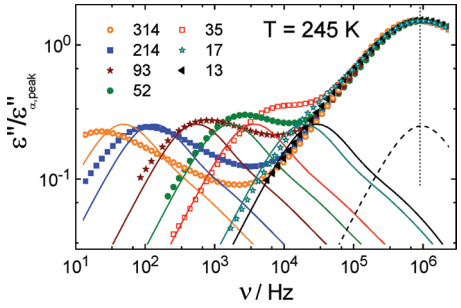

Figure 2. Dielectric loss spectra recorded at $T = 245$ K for a wide range of chain lengths are represented by the symbols. The amplitudes of the data are normalized with respect to the maximum of the α-peak. The dashed lines reflect a peak corresponding to a single relaxation time τ_N. The solid lines are calculations based on τ_N using eq 3. They describe the normal mode contributions very well for molecular weights for which entanglement effects do not occur.

The ν^1 region, which is seen for $N = 17$, is usually masked by conductivity effects arising from the transport of impurity ions. However, after application of a dc bias of 20 V for 2 h at 300 K the effective conductivity could be reduced by about 1 decade for each of the samples shown in Figure 1. Similar electrical purging effects are well-known in the field of polymers.[13,46−48]

To gain a more complete overview on the evolution of the polymer dynamics, in Figure 2 we present dielectric loss spectra for $N = 13-314$ at 245 K, a temperature at which segmental and normal modes are simultaneously visible in the accessible frequency window. The data are normalized with respect to the peak height of the segmental mode but not scaled as far as their peak frequency is concerned. This means that the average time scale of the segmental dynamics is practically unaffected by the length of the chain. The normal mode appears only as a weak feature close to the segmental peak at $N = 13$, then separates more from the later as the chain length is successively increased, and finally evolves into a clearly discernible feature for larger N.

It is instructive to compare these data with calculations based on the Rouse model which is expected to hold if the chain is Gaussian. In other words, if it obeys random walk statistics.[49] The bead−spring model yields the following expression for the correlation function in terms of the end-to-end vector $\vec{R}_{ee}$ relating to the dielectric normal mode

$$\langle \vec{R}_{ee}(0)\vec{R}_{ee}(t)\rangle \propto N \sum_{\substack{k=1 \\ \text{odd}}}^{N} \frac{1}{k^2} \exp(-t/\tau_k) \qquad (1)$$

Here the sum runs over the odd Rouse modes if the dipole moment is aligned along the chain contour. Because of the k^{-2} factor, the sum converges rapidly. The time scale of the kth order Rouse mode is

$$\tau_k = \frac{\gamma}{\zeta} 4 \sin^{-2}\left(\frac{k\pi}{2N}\right) \qquad (2)$$

where ζ denotes the monomeric friction coefficient and γ the effective spring constant associated with a Rouse bead, respectively. The only free parameter of this model as given by eqs 1 and 2 is thus γ/ζ. As a fit parameter we may therefore

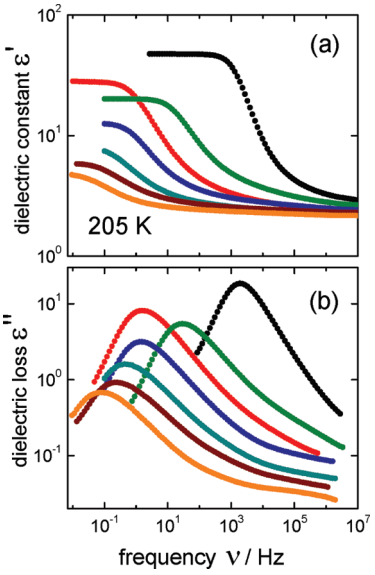

Figure 3. (a) Dielectric constant $\varepsilon'(\nu)$ and (b) dielectric loss $\varepsilon''(\nu)$ for $N = 1, 2, 3, 7, 13, 93$, and 314 at 205 K, a temperature at which the segmental relaxation is entirely in the experimental frequency window. The dispersion step and the loss peak amplitude decrease monotonously with increasing N. It is clearly seen that the relaxation rate of 2PG is exceptional.

choose a single time scale, i.e., that of the highest order Rouse mode, τ_N, which corresponds to the relaxation time of a single Rouse bead. For our calculations we used the same τ_N for all N, and for simplicity we identify τ_N with τ_α; see also ref 37. The Fourier transform of eq 1 then yields

$$\varepsilon'' \propto \sum_{\substack{k=1 \\ \text{odd}}}^{N} \frac{1}{k^2}\left[1 + 2\pi i\nu\tau_N \sin^{-2}\left(\frac{k\pi}{2N}\right)\right]^{-1} \qquad (3)$$

The solid lines in Figure 2 are the results of these calculations. The positions of the maxima agree best with the experimental NM peaks at intermediate molecular weights: On the one hand, for large $M_w > M_e$, corresponding to $N > 90$, entanglement effects lead to an enhanced slow down of the normal mode.[9] For very small chain lengths the Gaussian approximation is expected to break down. For PPG the molecular weight below which this happens is quite small.[37] Finally, Figure 2 shows that the shapes of the measured NM peaks appear broader than the Rouse calculations, as is typically observed also for other type A polymers.[50]

B. Segmental Dynamics for Variable Chain Lengths. In order to appreciate how the segmental relaxation in PPG evolves as a function of the chain length, Figure 3 displays the dielectric constants $\varepsilon'(\nu)$ and the dielectric losses $\varepsilon''(\nu)$ at $T = 205$ K for samples with $N = 1, 2, 3, 7, 13, 93$, and 314. In frame (b) of this figure one recognizes that the loss peak amplitudes and the peak frequencies for the α-process vary monotonously with N, and in frame (a) corresponding observations can be made for $\varepsilon'(\nu)$. However, from Figure 3 it is obvious that there is one exception: the relaxation of 2PG proceeds comparatively slow. Although we are not the first ones to point out this nonmonotonous behavior on the basis of dielectric measurements,[44] previously it was believed that it is the relaxation of 3PG which is exceptional.[51]

In order to check for a possible nonmonotonous N dependence with a different technique, we measured ^{13}C NMR spin−lattice relaxation times for PG, 2PG, and 3PG using

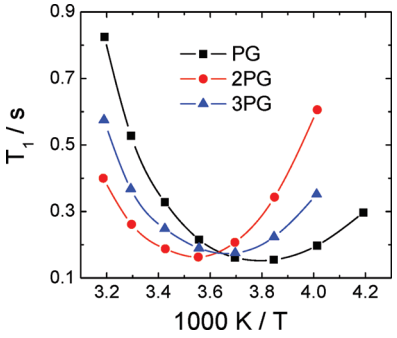

Figure 4. Temperature dependence of the ^{13}C NMR spin−lattice relaxation times for PG, 2PG, and 3PG (determined from the sum of the CH and the CH_2 carbon signals in the chemical shift range of 65−78 ppm). The T_1 minimum which shows up at the highest temperature corresponds to 2PG, i.e., not to the largest molecule. The lines are guides to the eye.

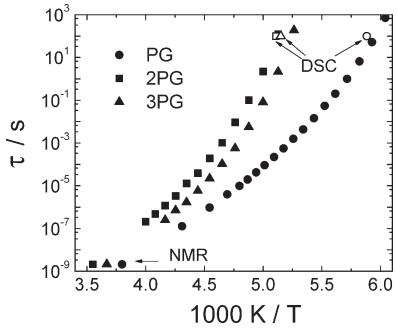

Figure 5. Arrhenius plot of the relaxation times for PG, 2PG, and 3PG. The data from calorimetry[44] and those from NMR (this work) are labeled. All others are calculated from dielectric loss maxima.

an inversion recovery sequence.[52] The methyl carbon signals appear at 17−20 ppm while methylene and methin carbons show up in the range of 65−78 ppm. The latter shift range was chosen for monitoring the recovery of the longitudinal magnetization, $M(t)$, as the integrated intensity of the CH and the CH_2 signals versus time. Then, $M(t)$ was fitted using an exponential function, $\propto \exp(-t/T_1)$. The temperature dependence of the resulting spin−lattice relaxation times, T_1, is plotted in Figure 4 for PG, 2PG, and 3PG. T_1 minima are observed for all samples. However, the T_1 minimum of 3PG is located between those of PG and 2PG.

The spin−lattice relaxation rate at the carbon site is governed by intramolecular dipole interaction and can be written as[53] $1/T_1 = K_{CH}[J(\omega_H - \omega_C) + 3J(\omega_C) + 6J(\omega_H + \omega_C)]$. Here $K_{CH} = (n/10)(\hbar\gamma_H\gamma_C/r^3)^2$ denotes the fluctuating part of the heteronuclear dipolar coupling of a ^{13}C spin to its n adjacent protons and r is the C−H internuclear distance. With the Larmor frequency ω_C (ω_H), the gyromagnetic ratio γ_C (γ_H) of the carbon (proton), and a typical C−H distance, $r = 1.08$ Å, one obtains $K_{CH} = n \times 2.27 \times 10^{10}$ s^{-2}. According to the approach of Bloembergen, Purcell, and Pound (BPP)[54] the spectral density is defined as $J(\omega) = \tau_C/[1 + (\omega\tau_C)^2]$ with τ_C denoting the molecular correlation time. If a distribution of correlation times is present, this expression has to be modified.[55] Without recourse to specific models one may just analyze the T_1 minimum for which $\omega_C\tau_C \approx 0.62$ holds. As shown in an Arrhenius representation, Figure 5, the resulting correlation times τ_C from NMR nicely agree with the time constants for the α-relaxation extrapolated from dielectric spectroscopy.

The special behavior of 2PG becomes particularly evident when plotting the dielectrically determined glass transition

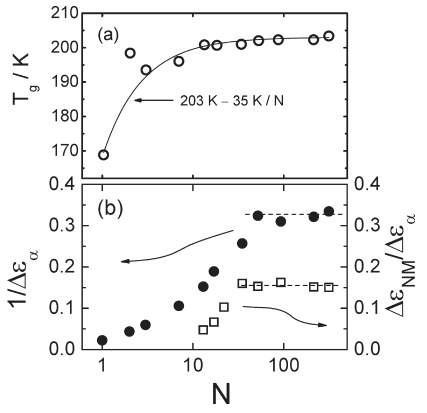

Figure 6. (a) Dielectrically determined T_g as a function of the number of repeat units N. All data, 2PG not taking into account, were fitted to yield the Fox−Flory equation given in this frame. The result is graphically represented by the line. (b) N-dependent dielectric relaxation strengths plotted as $1/\Delta\varepsilon_\alpha$ (circles) and as $\Delta\varepsilon_{NM}/\Delta\varepsilon_\alpha$ (squares). As a function of the molecular weight these quantities saturate at 0.33 ± 0.02 and 0.16 ± 0.01, respectively, as highlighted by the lines. The lines are drawn to guide the eye. $\Delta\varepsilon_{NM}/\Delta\varepsilon_\alpha$ is independent of N for $N > 30$. This independence marks the applicability of Gaussian statistics.

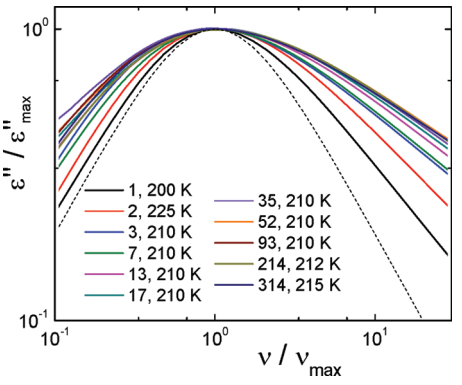

Figure 7. Dielectric losses in the segmental relaxation regime as scaled with respect to the peak frequency ν_{max} and the peak amplitude ε''_{max} are represented as solid lines. The data reveal a continuous broadening on the high-frequency side for increasing chain length. On the low-frequency side the peak broadens continuously for $N \leq 35$, then narrows, and finally turns N-independent. Note that for large N the normal mode ceases to interfere with the α-process.[37] For comparison, $\varepsilon''(\nu)$ calculated for a system with a single relaxation time (Debye case) is included (dashed line).

temperatures T_g as a function of the chain length. Here T_g is defined via $T(\tau_\alpha = 10^2$ s), which in some cases involved a slight extrapolation. The molecular weight dependence of T_g for all our samples is summarized in Figure 6a. Except for $N = 2$, it can be described by the Fox−Flory equation,[56] $T_g(N) = T_g(N\rightarrow\infty) - \Delta T/N$ with $T_g(N\rightarrow\infty) = 203$ K and $\Delta T = 35$ K. The overall trend contrasts with the previously offered conjectures that the relaxation of the 3PG might be too fast (see e.g., ref 44). The current data confirm that 2PG behaves different. We suppose that this may arise from an enhanced tendency to form hydrogen-bonded aggregates for this system.

Notwithstanding the nonmonotonous behavior of the mean time scales of the segmental relaxation, the high-frequency exponent of the associated loss peaks evolves in a smooth manner for all N. This becomes obvious from Figure 7 where we plot the scaled dielectric losses measured at temperatures chosen so that the α-peak frequencies are close to 10 Hz. The increase of the spectral width with increasing N appears plausible because the increase of the chain length may be expected to lead to a greater diversity of local environments.[57] For $N \geq 13$ the vertical shift applied for the ε''_{max} scaling in Figure 7 was within a factor of 2 for all systems. However, when considering all chain lengths the dispersion strength increased significantly for small N. Consequently, $1/\Delta\varepsilon_\alpha$ becomes very small when in this limit (cf. Figure 6b).

C. Relaxations Faster Than the Segmental Dynamics. Figure 8 contains dielectric loss spectra at temperatures close to and below T_g for samples with $N = 7$, 17, and 314. On the high-frequency flank of the segmental or α-relaxation peak two more relaxations are recognized. They are labeled with β and γ according to their frequency position. The relaxation times of these peak maxima are collected in an Arrhenius plot (Figure 9) for all N and are compared with τ_α. Similar representations were obtained previously for smaller N.[42,43] It is remarkable that the relaxation process β exhibits almost the same temperature-dependent relaxation times for all samples.[21] Except for $N < 7$ the same is true for the process labeled here as γ. To clarify the nature of these processes, dielectric pressure and aging studies were carried out.[43,58] It was reported that process β conforms to Ngai's coupling scheme and thus was occasionally classified as a "genuine Johari−Goldstein process",[59] while process γ may be related to the

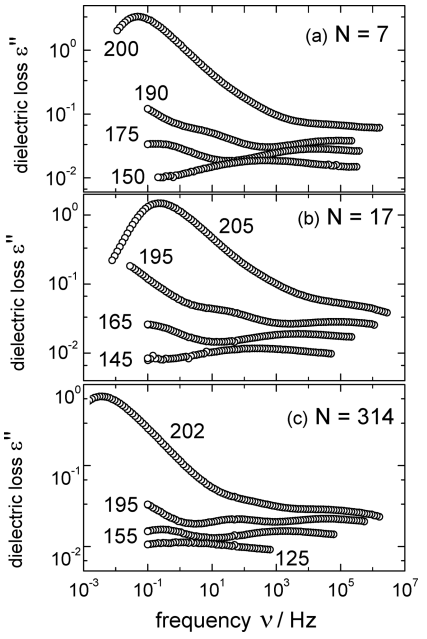

Figure 8. Dielectric losses for PPG with $N = 7$, 17, and 314 repeat units including spectra recorded for several temperatures (in Kelvin) below T_g. One observes the presence of two low-amplitude peaks. The one at lower frequencies is termed peak β, and the one at higher frequencies is termed peak γ.

presence of H-bonds.[43] It could be described within the "minimal model" of Dyre and Olsen.[60]

Next we show experimentally that the strength of process β is related to the presence of water. To this end we first measured reference spectra of a sample with $N = 314$ at 260 K and at 195 K. Then we heated this sample to 473 K and kept it there for about 1 h. After cooling to 260 K, we obtained the same spectrum as before (within experimental error) (cf. Figure 10), demonstrating that the segmental and the normal mode relaxations remain practically unaffected by this procedure. The spectra subsequently recorded at 195 K show that peak γ is also unaltered while peak β has significantly lost intensity. With prior heat treatment at 423 K for 1 h the loss of intensity is weaker. We also mention that the strength of peak β can be enhanced by exposing the sample to air at

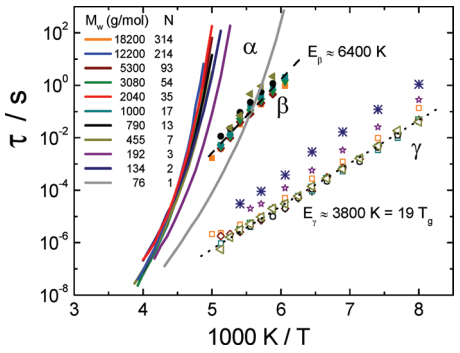

Figure 9. Compilation of relaxation times of PPG. The solid lines represent the structural relaxation time τ_α, the filled symbols reflect the time constants of peak β, and the open symbols and crosses represent those of peak γ. The other lines correspond to Arrhenius laws $\tau = \tau_0 \exp(E/T)$ (dashed line: process β; dotted line: process γ). The activation energies E_β and E_γ are given in temperature units and/or with respect to $T_g(N\rightarrow\infty)$. The pre-exponential factor is $\tau_0 = 10^{-15}$ s for both processes.

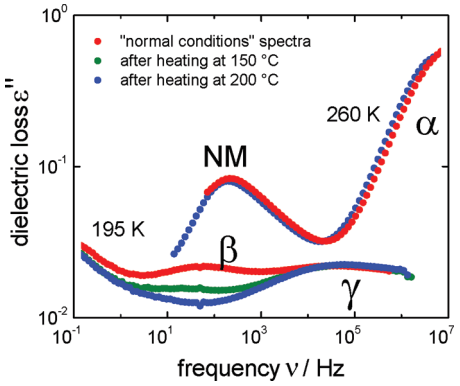

Figure 10. Dielectric loss spectra of a sample with $N = 314$ prior and subsequent to a heat treatment at 150 and at 200 °C. The spectra recorded at 260 K document that an exposure of the sample to relatively high temperatures has no significant effect on the normal-mode and on the segmental relaxation. The spectra taken at 195 K document that process γ is also unaffected by this procedure but that it reduces the intensity of peak β significantly.

room temperature for times longer than about 1 day. Since the activation energy of process β, $E_\beta \approx 6400$ K, is similar to that found in many water-containing systems,[61] this is a strong hint that peak β is related to a hydration of the PPG chain.

Process γ exhibits a lower activation energy E_γ which is the same for all samples with $M_w \geq 455$ g/mol (or $N \geq 7$). The value of E_γ is close to 20 T_g and thus similar to that usually observed for secondary relaxation processes in molecular glass formers.[62]

D. Polymer Chains as Molecular Rulers. The peak frequencies of the normal and of the segmental modes, or more precisely the corresponding time scales, are collected in Figure 11 for $N \geq 17$. As suggested by the results shown in Figure 9, the segmental relaxation times τ_α for all polymers agree with each other. As noted previously[19] for PPG τ_α tends to become equal to the time scale τ_{NM} corresponding to the normal mode peak near the low-temperature end of the pattern shown in Figure 11. The frequency at which the dynamics of both processes merge was given as $\log_{10}(\nu_\alpha/\text{Hz}) = 19.82 - 7.55 \log_{10}[M_w/(\text{g/mol})]$ for PPG and PI.[19] Our present data conform to this relationship for high M_w. In ref 19 it was suggested that at the merging temperature the length scale associated with the normal mode may match that of the segmental mode.

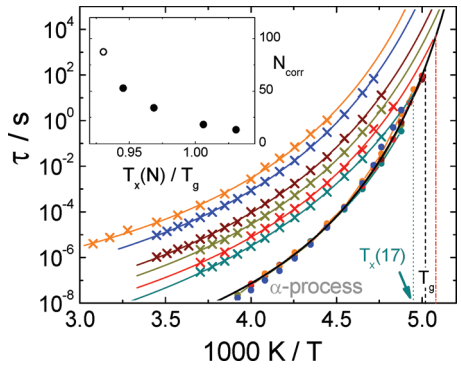

Figure 11. Arrhenius plot of the normal-mode and of the segmental relaxation times for PPG with $N \geq 17$. In this range τ_α follows a quasi-universal, N-independent behavior, while τ_{NM} increases with increasing chain length at a given temperature. The merging of the τ_α with the τ_{NM} trace occurs at a temperature $T_x(N)$, which is highlighted by the dotted line for $N = 17$ and by the dashed-dotted line for $N = 35$. The dashed line marks $T_g = T_g(N\rightarrow\infty)$. In the inset the merging temperature $T_x(N)/T_g(N\rightarrow\infty)$ is plotted for the different chain lengths N in a way to emphasize that the number of correlated segments increases upon cooling through the glass transition. One recognizes that near T_g one has $N_{corr} \approx 20$. The point corresponding to the polymer with $N = 93$, which requires substantial extrapolation, is represented by an open symbol.

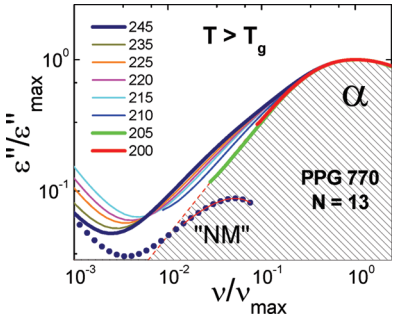

Figure 12. Dielectric loss of the 13-mer scaled with respect to height and frequency of the α-peak. The shape of the low-frequency flank of the segmental relaxation is highlighted by the shaded area. The low-frequency flank of the α-peak is the same as the one observed for systems with higher N, for which normal mode and segmental mode are better separated.[37] The data at 245 K indicate the existence of excess intensity which after subtraction of the loss due to the α-process yields a normal-mode peak. This peak, which is represented by the dots, is characterized by a very small intensity. When lowering the temperature down to $T_x \approx 205$ K, the excess intensity vanishes; in other words, the two relaxation modes have coalesced.

Here, by observing that the merging temperature, T_x, decreases as a function of increasing molecular weight, we take this argument one step further: Along the α-trace which is identical for all polymers with $N > 13$ we may read off the number of repeat units and thus estimate a length scale from $T_x(N)$. The results are shown in the inset of Figure 11 where we plot N versus the reduced temperature $T_x(N)/T_g(N\rightarrow\infty)$. It should be noted that while the data point for $N > 90$ requires a substantial extrapolation this is not the case for smaller N.

As an example for the directly observable coalescence of modes we show scaled dielectric losses for a sample with $N = 13$ in Figure 12. At high temperatures the normal mode shows up as a shoulder on the low-frequency side of the α-process. The latter exhibits the same slope in a wide range of molecular weights and is emphasized by the dashed line in Figure 12. Therefore, one may subtract the contribution of the segmental mode and thus render the normal mode visible

as a peak. Upon cooling the signature of the normal mode becomes weaker, and near 205 K it is no longer discernible; i.e., it has coalesced with the α-process.

Returning to the inset of Figure 11, one recognizes that $T_g(N\rightarrow\infty)$ and $T_x(N_\alpha)$ are about the same if one chooses $N_\alpha \approx 20$. To calculate a typical length scale λ from the number of repeat units $N_{corr} \approx N_\alpha$ one may use the characteristic ratio which for PPG is $C_\infty = 5.05$.[63] The numbers $13 \leq N \leq 93$ in the inset of Figure 11 correspond to $\lambda^2 = C_\infty N l^2$ with λ ranging from 2.9 to 7.8 nm if one uses $l = 3.58$ Å for the scale of the monomer unit.[64] The Gaussian approximation, as signaled by the N independence of $\Delta\varepsilon_{NM}/\Delta\varepsilon_\alpha$, is reached only for $N \geq 30$ (ref 37). Therefore, the length scale calculated for systems with $13 < N < 30$ may be slightly smaller than just estimated. Nevertheless, our results show that near T_g (where $N_{corr} \approx 20$) the cooperativity length characterizing the α-process of PPG is ~4 nm. The number of correlated segments is similar to that previously reported from dielectric investigations of polyisoprene[19] and from NMR studies of poly(vinyl acetate).[65,66] Furthermore, the associated length scale is consistent with estimates based on a mesoscopic mean-field model applied to the analysis of polymeric and molecular glass formers[67] and on measurements of higher order susceptibilities on such systems.[68] The fact that dynamic fluctuations of molten systems can become frozen in the glassy state was also frequently exploited to detect heterogeneity length scales in polymers and other systems.[69−71]

IV. Discussion

A. Dielectric Determination of the Characteristic Ratio. At a given temperature the relaxation strengths of the normal mode and of the α-process may be estimated using the Curie laws $\Delta\varepsilon_{NM} = N_{pol}\mu_{NM}^2/(3\varepsilon_0 k_B T)$ and $\Delta\varepsilon_\alpha = N_s\mu_\perp^2/(3\varepsilon_0 k_B T)$, respectively.[72,73] In the equations, ε_0 is the permittivity of free space and N_{pol} and N_s are the number density of the polymer chains and of the segments, respectively. $\mu_\perp$ is the absolute value of the monomeric dipole moment oriented perpendicular to a chain segment, and μ_{NM} is the absolute value of the mean end-to-end dipole moment of the chain. The latter is proportional to the polymer's mean end-to-end distance, R_{ee}, which can be estimated, e.g., using the model of freely rotating chains as[74]

$$R_{ee}^2 = Nl^2\left[\frac{1+\cos\theta}{1-\cos\theta} - \frac{2\cos\theta(1-\cos^N\theta)}{N\quad(1-\cos\theta)^2}\right] \qquad (4)$$

where θ denotes the bond angle. For sufficiently long chains the second term within the square brackets vanishes, and in this limit the characteristic ratio $C_\infty = R_{ee}^2/(Nl^2)$ is recovered.[75] Furthermore, since the product $N_{pol}N$ equals the density of the repeat units, N_s, we can write for the normal mode

$$\Delta\varepsilon_{NM} = N_s\mu_\parallel^2 C_\infty/(3\varepsilon_0 k_B T) \qquad (5)$$

Here $\mu_\parallel$ is the parallel-to-the-contour dipole moment per monomeric unit. Hence, the ratio $\Delta\varepsilon_{NM}/\Delta\varepsilon_\alpha$ should be constant for large N.[37,76,77] By combining eq 5 with the Curie law for $\Delta\varepsilon_\alpha$, we obtain a quantitative expression for this ratio from

$$\frac{\Delta\varepsilon_{NM}}{\Delta\varepsilon_\alpha} = C_\infty\frac{\mu_\parallel^2}{\mu_\perp^2} \qquad (6)$$

For PPG our experiments yield $\Delta\varepsilon_{NM}/\Delta\varepsilon_\alpha = 0.16 \pm 0.01$ (see Figure 6b or ref 37). Together with $C_\infty = 5.05$ (ref 63) eq 6 predicts $\mu_\parallel/\mu_\perp = 0.18$. This ratio agrees perfectly with literature values ($\mu_\parallel \approx 0.18$ D, $\mu_\perp \approx 1$ D).[78] Conversely, if the dipole moments are known, eq 6 can be used to determine C_∞.[79] Thus, information about the stiffness of the chain can be gained by simply measuring the ratio of the dielectric strengths of the two relaxation processes, preferably at a temperature much higher than T_g and for systems with reasonably long chains.

B. Transverse Dipole Moments in the Sub-Gaussian Regime. The strong decrease of $1/\Delta\varepsilon_\alpha$ (Figure 6b), hence strong increase of $\Delta\varepsilon_\alpha$ for $N\rightarrow 1$, suggests that a contribution to the amplitude of the segmental response should occur which was not discussed so far. For small-length type A polymers for which the Gaussian approximation is *not* valid, there will be a finite dipole moment oriented perpendicular to the end-to-end dipole moment axis. Hence, for decreasing N one expects that the amplitude of the α-process increases at the expense of the strength of the normal mode.

For chains in the Gaussian regime only the transversal-to-chain component of the segmental dipole moment contributes to the α-process, while it is the *total* molecular dipole moment, $\vec{\mu}_{tot} = \vec{\mu}_\parallel + \vec{\mu}_\perp$, which plays this role for the monomeric melt. The increased dispersion strength in the oligomeric regime is expected to be the more pronounced for larger ratios of $\mu_\parallel/\mu_\perp$. Hence, while $\mu_\parallel/\mu_\perp$ and thus the normal mode amplitude relative to that of the segmental peak is relatively small for PPG, more pronounced effects can be expected for systems such as oligo(isoprene)[12,76] or oligo(lactide).[15]

C. Encroachment of Normal and Segmental Modes. According to the classical theory of polymers, the relaxation times for the chain dynamics depends mainly on the monomeric friction coefficient; hence, practically the same T dependence is expected for τ_α and for τ_{NM}. However, experimentally it is generally observed that the temperature dependence of the segmental mode is much stronger than the one of the normal mode.[19,7] Thus, in harmony with previous results for PPG,[19] Figure 11 documents that also for this polymer the segmental and the normal modes behave differently in a way that they tend to merge toward low temperatures.

The calculation of the Rouse spectrum shown in Figure 2 was carried out by identifying at 245 K the highest order Rouse mode, τ_N, with the segmental relaxation time, τ_α. In view of the experimental observation of a temperature-dependent ratio of $\tau_1 \approx \tau_{NM}$ to τ_α this identification may seem fortuitous. To see that this is not the case, let us point out that it has arisen because the number N of Rouse segments appearing in eq 2 and the number of repeat units were more or less tacitly assumed to be the same. However, in the framework of our interpretation in eq 2 the variable N should be replaced by N/N_{corr} to take into account the correlation of segments that characterizes the segmental motion. The modified equation thus reads $\tau_N = \tau_1 \sin^2[(\pi N_{corr}/(2N)]$. Then, for each chain length the condition $N = N_{corr}$ is fulfilled at the intersection points [temperatures $T_x(N)$] in Figure 11, and the merging tendency of τ_{NM} and τ_α just reflects the increase of N_{corr} upon cooling, while the temperature independence of the ratio τ_1/τ_N that follows from eq 2 can be maintained.

Several other arguments were previously advanced to explain the tendency of segmental and normal modes to merge toward low temperatures.[80] One of them is based on experiments showing that the self-diffusion coefficient and the normal mode relaxation rate of PPG exhibit essentially the same T dependence.[7,25] Since the α-process corresponds to the rotational dynamics of the segments around the polymer backbone, the different temperature dependences of the α and NM-processes, becoming significant below about 230 K,

were interpreted to arise from a translational−rotational decoupling.[81] However, light scattering results indicate that above 210 K the "segmental reorientation is strongly coupled to the segmental center-of-mass translational motion",[26] which is at variance with the notion of a decoupling. As an alternative interpretation the different temperature dependences of τ_α and τ_{NM} were found to be consistent with the different stretchings of the involved processes within Ngai's coupling model.[82] In the spirit of previous mechanical spectroscopy work,[83] Ngai et al. additionally rationalized the "encroachment" of the two processes by demonstrating experimentally that $\Delta\varepsilon_{NM}$ of PPG (with a molecular weight of about 1000 g/mol) strongly decreases when the mode coalescence is closely approached upon coming from high temperatures. Our analyses for systems with similar chain lengths (N = 17 and 22) confirm that close to the merging point $\Delta\varepsilon_{NM}$ decreases as $\Delta\varepsilon_\alpha$ gets larger (not shown).

The merging is most directly observed for the sample with N = 13. As discussed in section III.D, the scaling of the dielectric loss in Figure 12 reveals that the normal mode contribution vanishes somewhat below 210 K. It is important to emphasize that the time constants for the merged, "surviving" process follow the same temperature dependence which characterizes the α-relaxation of all systems with $N > 13$. Since this suggests that the relaxation rates of the segmental and the normal modes do not depend on each other, we may conclude that the two processes are statistically independent even for N = 13.

D. Impact of Hydrogen Bonding and Comparison with Other Polymer Systems. PPG, HO−[$CH_2CH(CH_3)O$]$_N$−H, features hydrogen bonds and is thus an interesting system to study. This polymer was even used to extrapolate to the case of water which would correspond to $N \rightarrow 0$.[84] In the present context, we wish to discuss how H-bonding in PPG affects its overall chain dynamics. Generally, for a given molecular weight hydrogen bonding can increase the effective chain length, e.g., leading to the "transient entanglement" effects mentioned above. These effects may explain the shift of the entanglement molecular weight, separating the nonreptation from the reptation regime, to relatively low values.[25,39,40] An interesting observation made in the short-chain regime is that the Rouse model remains applicable for the description of the relaxation times of the normal modes down to a surprisingly low molecular weight, M_w = 790 g/mol.[31,37]

With increasing chain length the glass-transition temperature of PPG saturates at only a few repeat units (see Figure 6a). In relation to the much stronger dependence of T_g on N for other polymer systems[85,86] for PPG the insensitivity of $T_g(M_w)$ can be explained by the formation of a hydrogen-bonded network.[18]

As seen in Figure 7, not only the position but also the shape of the α-peak for N larger than about 7 does not change much, demonstrating a relative insensitivity of the local environment on the chain length. In fact, the peak amplitude (the relaxation strength) of the structural relaxation changes significantly only for small and intermediate N (cf. Figure 6b). This variation of $\Delta\varepsilon_\alpha$ with N, obvious also from other studies,[27] may tentatively be connected to the presence of hydrogen bonds, since they facilitate static cross-correlations between adjacent segments. For small chains the number of terminal H and OH groups is higher; thus, a stronger contribution to the relaxation strength of the segmental response is expected here. This may explain the behavior of $1/\Delta\varepsilon_\alpha(N)$ in Figure 6b. For systems with N larger than 30, $1/\Delta\varepsilon_\alpha$ saturates to a value close to 3, indicating that in this range the hydrogen bonds cease to play an important role for the segmental dynamics.

V. Conclusions

Using dielectric spectroscopy, we investigated the normal-mode and the segmental dynamics as well as several low-temperature relaxation processes in PPG for a large range of chain lengths. The samples were subjected to an electrical cleaning procedure. This allowed us to identify the slowest dipolar end-to-end mode of the 17-mer as a change of slope on the low-frequency side of the dielectric loss peak. For intermediate molecular weights the position of the normal-mode maxima could be described semiquantitatively without free parameters using calculations via the Rouse model. Our systematic investigation of the molecular weight effects, also using ^{13}C spin−lattice relaxation, demonstrated that the α-relaxation of 2PG is anomalously slow and not, in contrast to previous contentions, that the dynamics of 3PG is too fast. The dispersion strength $\Delta\varepsilon_\alpha$ and the ratio of the static dielectric constants, $\Delta\varepsilon_{NM}/\Delta\varepsilon_\alpha$, exhibit an interesting dependence on the degree of polymerization. The ratio of dispersion steps increases with increasing N up to about $N \approx 30$ and then turns to a constant, thus signaling the onset of Gaussian chain statistics. The numerical value of this constant, $\Delta\varepsilon_{NM}/\Delta\varepsilon_\alpha = 0.16$ for PPG, was demonstrated to allow one to extract the characteristic ratio C_∞ provided that the longitudinal and transverse segmental dipole moments are known, or vice versa.

Two sub-T_g relaxation processes were found in all samples with $N \geq 7$. Using a heat treatment at temperatures above 100 °C the slower of the two processes (termed β) could be significantly reduced in intensity. This finding, together with the observation that its relaxation time can be described by an activation energy E_β which corresponds to the energy required to break two hydrogen bonds, suggests that its occurrence is associated with the presence of water.

An important observation is the (incipient) coalescence of normal and segmental modes. It occurs for $13 \leq N \leq 35$ at a temperature $T_x(N)$ in the vicinity of T_g and for larger chains at somewhat lower temperatures. The coalescence of modes was taken to signal a similarity of the involved length scales. Thus, we interpret $T_x(N)$ as the temperature at which the cooperativity length scale of the α-process in a polymer with N repeat units is about the same as the end-to-end distance for the corresponding chain length. The change in the number of correlated segments is considered as a temperature effect and not a molecular weight effect. Thus, employing the normal mode as a molecular ruler, we find that the cooperativity length increases with decreasing temperatures reaching a length scale of about 4 nm near T_g.

Acknowledgment. We thank Andreas Schönhals for fruitful discussions, Bayer Co. for kindly providing the samples with N = 214 and 314, and Axel H. E. Müller for the MALDI-TOF characterization of the samples.

References and Notes

(1) Baur, M. E.; Stockmayer, H. *J. Chem. Phys.* **1965**, *43*, 4319–4325.
(2) Beevers, M. S.; Elliott, D. A.; Williams, G. *Polymer* **1980**, *21*, 13–20.
(3) Adachi, K.; Kotaka, T. *Macromolecules* **1987**, *20*, 2018–2023.
(4) Jacobsson, P.; Börjesson, L.; Torell, L. M. *J. Non-Cryst. Solids* **1991**, *131−133*, 104–108.
(5) Ding, Y.; Kisliuk, A.; Sokolov, A. P. *Macromolecules* **2004**, *37*, 161–166.
(6) Kariyo, S.; Gainaru, C.; Schick, H.; Brodin, A.; Rössler, E. A. *Phys. Rev. Lett.* **2006**, *97*, 207803.
(7) Schönhals, A. In *Broadband Dielectric Spectroscopy*; Kremer, F., Schönhals, A., Eds.; Springer: Berlin, 2003; Chapter 7.
(8) de Gennes, P. G. In *Scaling Concepts in Polymer Physics*; Cornell University Press: Ithaca, NY, 1979.
(9) Doi, M.; Edwards, S. F. *The Theory of Polymer Dynamics*; Clarendon: Oxford, 1986.

(10) Riande, E.; Diaz-Calleja, R. *Electrical Properties of Polymers*; Marcel Dekker: New York, 2004.
(11) Williams, G. *Macromol. Symp.* **2009**, *286*, 1–19.
(12) Adachi, K.; Kotaka, T. *Prog. Polym. Sci.* **1993**, *18*, 585–622.
(13) Se, K.; Adachi, K.; Kotaka, T. *Polym. J.* **1981**, *13*, 1009–1017.
(14) Casalini, R.; Roland, C. M. *Macromolecules* **2005**, *38*, 1779–1788.
(15) Mierzwa, M.; Floudas, G.; Dorgan, J.; Knauss, D.; Wegner, J. *J. Non-Cryst. Solids* **2002**, *307*−*310*, 296–303.
(16) Further examples are given in: Hirose, Y.; Adachi, K. *Polymer* **2005**, *46*, 1913–1920.
(17) Hayakawa, T.; Adachi, K. *Polymer* **2001**, *42*, 1725–1732.
(18) Engberg, D.; Schüller, J.; Strube, B.; Sokolov, A. P.; Torell, L. M. *Polymer* **1999**, *40*, 4755–4761.
(19) Schönhals, A.; Schlosser, E. *Phys. Scr.* **1993**, *T49*, 233–236. Schönhals, A.; Schlosser, E. *Prog. Colloid Polym. Sci.* **1993**, *91*, 158–161.
(20) Mattsson, J.; Bergman, R.; Jacobsson, P.; Börjesson, L. *Phys. Rev. Lett.* **2003**, *90*, 075702.
(21) Mattsson, J.; Bergman, R.; Jacobsson, P.; Börjesson, L. *Phys. Rev. Lett.* **2005**, *94*, 165701.
(22) Moon, I. K.; Jeong, Y. H.; Furukawa, T. *Thermochim. Acta* **2001**, *377*, 97–104.
(23) Mel'nichenko, Y. B.; Schüller, J.; Richert, R.; Ewen, B.; Long, C.-K. *J. Chem. Phys.* **1995**, *103*, 2016–2024.
(24) Fleischer, G.; Helmstedt, M.; Alig, I. *Polym. Commun.* **1990**, *31*, 409–411.
(25) Appel, M.; Fleischer, G.; Kärger, J.; Chang, I.; Fujara, F.; Schönhals, A. *Colloid Polym. Sci.* **1997**, *275*, 187–191.
(26) Wang, C. H.; Fytas, G.; Lilge, D.; Dorfmüller, T. *Macromolecules* **1981**, *14*, 1363–1370.
(27) Ko, J.-H.; Kojima, S. *Phys. Lett. A* **2004**, *321*, 141–146.
(28) Yano, S.; Rabalkar, R. R.; Hunter, S. P.; Wang, C. H.; Boyd, R. H. *J. Polym. Sci., Polym. Phys. Ed.* **1976**, *14*, 1877–1890.
(29) (a) Yoshihara, A.; Sato, H.; Kojima, S. *Jpn. J. Appl. Phys.* **1996**, *35*, 2925–2929. (b) Yoshihara, A.; Sato, H.; Kojima, S. *Prog. Theor. Suppl.* **1996**, *126*, 423–426. (c) Kojima, S.; Sato, H.; Yosihara, A. *J. Phys.: Condens. Matter* **1997**, *9*, 10079–10085.
(30) Alig, I.; Grigorev, S. B.; Manucarov, Yu. S.; Manucarova, S. A. *Acta Polym.* **1986**, *37*, 698−702 and 733−736.
(31) Cochrane, J.; Harrison, G.; Lamb, J.; Phillips, D. W. *Polymer* **1980**, *21*, 837–844.
(32) Swenson, J.; Köper, I.; Telling, M. T. F. *J. Chem. Phys.* **2002**, *116*, 5073–5079.
(33) Vogel, M.; Torbrügge, T. *J. Chem. Phys.* **2007**, *126*, 204902.
(34) Roland, C. M.; Psurek, T.; Pawlus, S.; Paluch, M. *J. Polym. Sci., Part B: Polym. Phys.* **2003**, *41*, 3047–3052.
(35) (a) Schönhals, A.; Stauga, R. *J. Non-Cryst. Solids* **1998**, *450*, 235–237. (b) Schönhals, A.; Stauga, R. *J. Chem. Phys.* **1998**, *108*, 5130–5136.
(36) Schwartz, G. A.; Bergman, R.; Swenson, J. *J. Chem. Phys.* **2004**, *120*, 5736−5744 and references cited therein.
(37) Gainaru, C.; Böhmer, R. *Macromolecules* **2009**, *42*, 7616–7618.
(38) Smith, B. A.; Samulski, E. T.; Yu, L. P.; Winnik, M. A. *Macromolecules* **1985**, *18*, 1901–1905.
(39) Heinrich, G.; Alig, I.; Donth, E. *Polymer* **1988**, *29*, 1198–1202.
(40) Alig, I.; Donth, E.; Schenk, W.; Horing, S.; Wohlfarth, C. *Polymer* **1988**, *29*, 2081–2086.
(41) Ahlström, P.; Wahnström, G.; Carlsson, P.; Schantz, S.; Brodin, A.; Maurer, F.; Torell, L. *Philos. Mag. B* **1998**, *77*, 699–707.
(42) Leon, C.; Ngai, K. L.; Roland, C. M. *J. Chem. Phys.* **1999**, *110*, 11585–11591.
(43) (a) Grzybowska, K.; Grzybowski, A.; Ziolo, J.; Paluch, M.; Capaccioli, S. *J. Chem. Phys.* **2006**, *125*, 044904. (b) Grzybowska, K.; Grzybowsky, A.; Ziolo, J.; Rzoska, S. J.; Paluch, M. *J. Phys.: Condens. Matter* **2007**, *19*, 376105.
(44) Köhler, M.; Lunkenheimer, P.; Goncharov, Y.; Wehn, R.; Loidl, A. arXiv:0810.5316v1, **2008**.
(45) Wagner, H.; Richert, R. *J. Phys. Chem. B* **1999**, *103*, 4071–4077.
(46) Osaki, S.; Uemura, S.; Ishida, Y. *J. Polym. Sci., Polym. Phys. Ed.* **1971**, *9*, 585–94.
(47) Nazemi, A.; Williams, G.; Attard, G. S.; Karasz, F. E. *Polym. Adv. Technol.* **1992**, *3*, 157–168.
(48) Gainaru, C.; Böhmer, R.; Williams, G., to be published.
(49) Rouse, P. E., Jr. *J. Chem. Phys.* **1953**, *21*, 1272–1280.
(50) Watanabe, H. *Macromol. Rapid Commun.* **2001**, *22*, 127–175.
(51) Note that according to ref 44 the calorimetric glass transition temperatures of 2PG and 3PG are rather similar.
(52) Vold, R. L.; Waugh, J. S.; Klein, M. P.; Phelps, D. E. *J. Chem. Phys.* **1968**, *48*, 3831–3832.
(53) Heatley, F. *Prog. Nucl. Magn. Reson. Spectrosc.* **1979**, *13*, 47–87.
(54) Bloembergen, N.; Purcell, E.; Pound, R. *Phys. Rev.* **1948**, *73*, 679–712.
(55) Connor, T. M. *Trans. Faraday Soc.* **1964**, *60*, 1574–1591.
(56) Fox, T.; Flory, P. J. *J. Polym. Sci.* **1954**, *14*, 315–319.
(57) Smooth molecular-weight-dependent broadening effects are more clearly revealed for PPG than for many other polymer systems. See, e.g.: Lusceac, S. A.; Gainaru, C.; Vogel, M.; Koplin, C.; Medick, P.; Rössler, E. A. *Macromolecules* **2005**, *38*, 5625–5633.
(58) Pawlus, S.; Hensel-Bielowka, S.; Grzybowska, K.; Zioło, J.; Paluch, M. *Phys. Rev.* **2005**, *71*, 174107.
(59) Ngai, K. L.; Paluch, M. *J. Chem. Phys.* **2004**, *120*, 857–873.
(60) Dyre, J.; Olsen, N. B. *Phys. Rev. Lett.* **2003**, *91*, 155703.
(61) Cerveny, S.; Alegria, A.; Colmenero, J. *Phys. Rev.* **2008**, *E 77*, 031803.
(62) Kudlik, A.; Benkhof, S.; Blochowicz, T.; Tschirwitz, C.; Rössler, E. A. *J. Mol. Struct.* **1999**, *479*, 201–218.
(63) Brandrup, J., Immergut, E. H. *Polymer Handbook*; John Wiley: New York, 1989.
(64) Ishikawa, T.; Teramono, A. *Polym. J.* **1974**, *6*, 207–215.
(65) Tracht, U.; Wilhelm, M.; Heuer, A.; Feng, H.; Schmidt-Rohr, K.; Spiess, H. W. *Phys. Rev. Lett.* **1998**, *81*, 2727–2730.
(66) Reinsberg, S. A.; Heuer, A.; Doliwa, B.; Zimmermann, H.; Spiess, H. W. *J. Non-Cryst. Solids* **2002**, *307*−*310*, 208–214.
(67) Chamberlin, R. V. *Phys. Rev. Lett.* **1999**, *82*, 2520–2523.
(68) Dalle-Ferrier, C.; Thibierge, C.; Alba-Simionesco, C.; Berthier, L.; Biroli, G.; Bouchaud, J.-P.; Ladieu, F.; L'Hôte, D.; Tarjus, G. *Phys. Rev.* **2007**, *E 76*, 041510.
(69) Moynihan, C. T.; Schroeder, J. *J. Non-Cryst. Solids* **1993**, *160*, 52–59.
(70) Masciovecchio, C.; Baldi, G.; Caponi, S.; Comez, L.; Di Fonzo, S.; Fioretto, D.; Fontana, A.; Gessini, A.; Santucci, S. C.; Sette, F.; Viliani, G.; Vilmercati, P.; Ruocco, G. *Phys. Rev. Lett.* **2006**, *97*, 035501.
(71) Hong, L.; Gujrati, P. D.; Novikov, V. N.; Sokolov, A. P. *J. Chem. Phys.* **2009**, *131*, 194511.
(72) Böttcher, C. J. F.; Bordewijk, P. *Theory of Electric Polarization I: Dielectrics in Static Fields*; Elsevier: Amsterdam, 1978.
(73) These relations are expected to hold best at high temperatures and for large N. Under these conditions static dipole correlations, sometimes parametrized using Kirkwood's g factor (see e.g., ref 10), should be small.
(74) Flory, P. J. *Statistical Mechanics of Chain Molecules*; Interscience Publishers: New York, 1969; Volkenstein, M. V. *Configurational Statistics of Polymeric Chains*; Interscience Publishers: New York, 1963.
(75) With $C_\infty \neq 1$ the expression just above eq (2) in ref 37 should read $\mu_{NM}^2 = C_\infty N_{s/pol} \mu_s^2$.This modification does not change the arguments advanced in that paper.
(76) Imanishi, Y.; Adachi, K.; Kotaka, T. *J. Chem. Phys.* **1988**, *89*, 7585–7592.
(77) Stühn, B.; Stickel, F. *Macromolecules* **1992**, *25*, 5306–5312.
(78) Stockmayer, W. H. *Pure Appl. Chem.* **1967**, *15*, 539–554.
(79) This determination implies that static dipole correlations are absent ($g = 1$), identical, or otherwise known for the segmental as well as for the normal mode processes.
(80) Ilan, B.; Loring, R. F. *Macromolecules* **1999**, *32*, 949–951.
(81) Decoupling effects are often discussed for simple molecular glass formers. See e.g.: Chang, I.; Fujara, F.; Geil, B.; Heuberger, G.; Mangel, T.; Sillescu, H. *J. Non-Cryst. Solids* **1994**, *172*−*174*, 248–255.
(82) Ngai, K. L.; Schönhals, A.; Schlosser, E. *Macromolecules* **1992**, *25*, 4915–4919.
(83) Ngai, K. L.; Plazek, D. J.; Deo, S. S. *Macromolecules* **1987**, *20*, 3047–3054.
(84) Mattsson, J.; Bergman, R.; Jacobsson, P.; Börjesson, L. *Phys. Rev. B* **2009**, *79*, 174205.
(85) Sokolov, A. P.; Novikov, V. N.; Ding, Y. *J. Phys.: Condens. Matter* **2007**, *19*, 205116.
(86) Abou Elfadl, A.; Kahlau, R.; Herrmann, A.; Novikov, V. N.; Rössler, E. A. *Macromolecules*, submitted.